OFFICE OF NAVAL RESEARCH

Grant No. N00014-90-J-1263

RCT Project 4133002---05

Technical Report #9

IN SITU SURFACE X-RAY SCATTERING OF METAL MONOLAYERS ADSORBED AT SOLID-LIQUID INTERFACES

by

M.F. Toney, J.G. Gordon and O.R. Melroy*

Prepared for Publication in the
SPIE Proceedings

*IBM Research Division, Almaden Research Center, 650 Harry Road
San José, California 95120-6099

REPORT DOCUMENTATION PAGE

1a. REPORT SECURITY CLASSIFICATION	1b RESTRICTIVE MARKINGS
2a. SECURITY CLASSIFICATION AUTHORITY	3 DISTRIBUTION / AVAILABILITY OF REPORT
2b. DECLASSIFICATION / DOWNGRADING SCHEDULE	
4. PERFORMING ORGANIZATION REPORT NUMBER(S) Technical Report #9	5. MONITORING ORGANIZATION REPORT NUMBER(S)
6a. NAME OF PERFORMING ORGANIZATION Physics Department University of Puerto Rico 6b OFFICE SYMBOL (If applicable)	7a NAME OF MONITORING ORGANIZATION
6c. ADDRESS (City, State, and ZIP Code) Río Piedras Puerto Rico 00931-3343	7b ADDRESS (City, State, and ZIP Code)
8a. NAME OF FUNDING / SPONSORING ORGANIZATION Chemistry Office of Naval Research 8b. OFFICE SYMBOL (If applicable) Code 472	9 PROCUREMENT INSTRUMENT IDENTIFICATION NUMBER RCT Project 4133002---05
8c. ADDRESS (City, State, and ZIP Code) Arlington Virginia 22217-5000	10 SOURCE OF FUNDING NUMBERS PROGRAM ELEMENT NO / PROJECT NO. / TASK NO / WORK UNIT ACCESSION NO

11. TITLE (Include Security Classification)
In Situ Surface X-Ray Scattering Metal Monolayers Adsorbed at Solid-Liquid Interfaces

12. PERSONAL AUTHOR(S) Michael F. Toney, Joseph G. Gordon and Owen R. Melroy

13a. TYPE OF REPORT	13b. TIME COVERED	14 DATE OF REPORT (Year, Month, Day)	15. PAGE COUNT
Summary	FROM _____ TO _____	11-09-91	11

16. SUPPLEMENTARY NOTATION

17 COSATI CODES			18. SUBJECT TERMS (Continue on reverse if necessary and identify by block number)
FIELD	GROUP	SUB-GROUP	

19 ABSTRACT (Continue on reverse if necessary and identify by block number)

The structure of the solid-liquid interface is of fundamental importance in chemistry, but progress in understanding this interface has been slow, due to the lack of in-situ probes that provide information at atomic scales. Recently, in-situ surface X-ray scattering measurements have provided insight into the microscopic nature of solid-liquid interfaces and this paper will discuss experiments on electrochemically deposited monolayers of Pb, Tl, and Bi on Ag and Au (111) electrodes.

20 DISTRIBUTION / AVAILABILITY OF ABSTRACT	21 ABSTRACT SECURITY CLASSIFICATION	
☒ UNCLASSIFIED/UNLIMITED ☐ SAME AS RPT ☐ DTIC USERS		
22a NAME OF RESPONSIBLE INDIVIDUAL Robert J. Nowak	22b TELEPHONE (Include Area Code) (202) 696-4410	22c. OFFICE SYMBOL Code 472

DD FORM 1473, 84 MAR 83 APR edition may be used until exhausted
All other editions are obsolete

SECURITY CLASSIFICATION OF THIS PAGE

Tl and Pb form two-dimensional (2D), incommensurate hexagonal solids that are compressed relative to bulk and rotated by 4-5° with respect to the substrate. As the applied electrode potential decreases, the in-plane atomic spacing also decreases, since the chemical potential of the monolayer increases. From these data, the 2D compressibility the monolayer can be calculated. We find that the compressibility is only slightly dependent on substrate, being smaller on Ag(111) than on Au(111). For Tl/Ag(111), the intensity of the Ag surface diffraction changes when the monolayer is adsorbed. This results from a substrate-induced modulation of the atomic positions in the incommensurate monolayer and we have quantified this modulation. Bi/Ag(111) forms an unusual structure: a rectangular lattice that is uniaxially commensurate with the hexagonal surface. There are two Bi adatoms per rectangular unit cell and one adatom is displaced from the centered position by 0.35 A. The commensurate Bi rows lie along the rows of three-fold hollow sites on the Ag(111) surface. This unusual structure reflects the tendency toward covalent bonding found in Bi and a fortuitous match between the atomic spacings of the Ag substrate and the close packed planes of bulk Bi. In contrast to Tl and Pb where the compressibility is isotropic, Bi/Ag(111) compresses anisotropically and this maintains the uniaxially commensurate structure.

Our results show that for these metal monolayer systems the adatom-adatom interactions determine the atomic structure of the monolayer and the adatom-substrate interactions only weakly affect this structure. Furthermore, the structure is not influenced by the presence of the large concentration of adsorbed water molecules or anions.

IN SITU SURFACE X-RAY SCATTERING METAL MONOLAYERS ADSORBED AT SOLID-LIQUID INTERFACES

Michael F. Toney
Joseph G. Gordon
Owen R. Melroy

IBM Research Division
Almaden Research Center
650 Harry Road
San Jose, California 95120-6099

ABSTRACT

The structure of the solid-liquid interface is of fundamental importance in chemistry, but progress in understanding this interface has been slow, due to the lack of in-situ probes that provide information at atomic scales. Recently, in-situ surface X-ray scattering measurements have provided insight into the microscopic nature of solid-liquid interfaces and this paper will discuss experiments on electrochemically deposited monolayers of Pb, Tl, and Bi on Ag and Au (111) electrodes.

Tl and Pb form two-dimensional (2D), incommensurate hexagonal solids that are compressed relative to bulk and rotated by 4-5° with respect to the substrate. As the applied electrode potential decreases, the in-plane atomic spacing also decreases, since the chemical potential of the monolayer increases. From these data, the 2D compressibility the monolayer can be calculated. We find that the compressibility is only slightly dependent on substrate, being smaller on Ag(111) than on Au(111). For Tl/Ag(111), the intensity of the *Ag surface diffraction* changes when the monolayer is adsorbed. This results from a substrate-induced modulation of the atomic positions in the incommensurate monolayer and we have quantified this modulation. Bi/Ag(111) forms an unusual structure: a *rectangular* lattice that is uniaxially commensurate with the *hexagonal* surface. There are two Bi adatoms per rectangular unit cell and one adatom is displaced from the centered position by 0.35 Å. The commensurate Bi rows lie along the rows of three-fold hollow sites on the Ag(111) surface. This unusual structure reflects the tendency toward covalent bonding found in Bi and a fortuitous match between the atomic spacings of the Ag substrate and the close packed planes of bulk Bi. In contrast to Tl and Pb where the compressibility is isotropic, Bi/Ag(111) compresses anisotropically and this maintains the uniaxially commensurate structure.

Our results show that for these metal monolayer systems the adatom-adatom interactions determine the atomic structure of the monolayer and the adatom-substrate interactions only weakly affect this structure. Furthermore, the structure is not influenced by the presence of the large concentration of adsorbed water molecules or anions.

In Situ Surface X-ray Scattering of Metal Monolayers Adsorbed at Solid-Liquid Interfaces

Michael F. Toney, Joseph G. Gordon, and Owen R. Melroy

IBM Research Division, Almaden Research Center
650 Harry Road, San Jose, California 95120-6099

ABSTRACT

The structure of the solid-liquid interface is of fundamental importance in chemistry, but progress in understanding this interface has been slow, due to the lack of in-situ probes that provide information at atomic scales. Recently, in-situ surface X-ray scattering measurements have provided insight into the microscopic nature of solid-liquid interfaces and this paper will discuss experiments on electrochemically deposited monolayers of Pb, Tl, and Bi on Ag and Au (111) electrodes.

Tl and Pb form two-dimensional (2D), incommensurate hexagonal solids that are compressed relative to bulk and rotated by 4-5° with respect to the substrate. As the applied electrode potential decreases, the in-plane atomic spacing also decreases, since the chemical potential of the monolayer increases. From these data, the 2D compressibility the monolayer can be calculated. We find that the compressibility is only slightly dependent on substrate, being smaller on Ag(111) than on Au(111). For Tl/Ag(111), the intensity of the *Ag surface diffraction* changes when the monolayer is adsorbed. This results from a substrate-induced modulation of the atomic positions in the incommensurate monolayer and we have quantified this modulation. Bi/Ag(111) forms an unusual structure: a *rectangular* lattice that is uniaxially commensurate with the *hexagonal* surface. There are two Bi adatoms per rectangular unit cell and one adatom is displaced from the centered position by 0.35 Å. The commensurate Bi rows lie along the rows of three-fold hollow sites on the Ag(111) surface. This unusual structure reflects the tendency toward covalent bonding found in Bi and a fortuitous match between the atomic spacings of the Ag substrate and the close packed planes of bulk Bi. In contrast to Tl and Pb where the compressibility is isotropic, Bi/Ag(111) compresses anisotropically and this maintains the uniaxially commensurate structure.

Our results show that for these metal monolayer systems the adatom-adatom interactions determine the atomic structure of the monolayer and the adatom-substrate interactions only weakly affect this structure. Furthermore, the structure is not influenced by the presence of the large concentration of adsorbed water molecules or anions.

I. INTRODUCTION

The atomic structure at the solid-liquid interface is of fundamental importance in electrochemistry, since this structure strongly affects the chemical and physical properties of the interface. Despite this, a determination of the structure of the solid-liquid interface has proved elusive. Surfaces inherently contain very few atoms. Hence, to obtain the required sensitivity, surface science has largely relied on probes that interact very strongly with matter. In addition to the high sensitivity, this approach has the added advantage of providing surface selectivity, since the probe does not penetrate far into the bulk substrate. Unfortunately, the same features which make these techniques so attractive for surface studies preclude their use outside ultrahigh vacuum (UHV), and thus, the techniques are unusable as in-situ probes of electrochemical interfaces. To date, most

successful in-situ studies have relied primarily on ultraviolet, visible or infrared radiation, since their propagation distances in many solutions are suitably large. These methods have provided valuable information on the type and possible orientation of interfacial species, but only indirectly indicate crystallographic structure.

X-ray diffraction has long been recognized as the most powerful technique for structure determination of three-dimensional (3D) matter, and in the past decade, much progress has been made in the application of X-ray diffraction to the study of two-dimensional (2D) adsorbed layers and surfaces.[1-3] The principal advantage of X-ray diffraction compared to more familiar surface structural tools, such as low-energy electron diffraction (LEED) and reflection high-energy electron diffraction (RHEED), is that X-rays interact weakly with matter. Thus, the kinematic theory of diffraction applies and the interpretation of intensities is greatly simplified compared to LEED and RHEED. The weak interaction of X-rays with matter provides an additional advantage for measurements of structures that are "buried" beneath a condensed phase or thin film, since it results in a large penetration depth. Therefore, X-rays can be used to probe buried interfaces, unlike most other surface-sensitive structural techniques.

Using surface X-ray scattering, substantial progress has recently made in determining, in-situ, the atomic structure of solid-liquid interfaces,[3-14] and this paper summarizes results of our investigations of electrochemically adsorbed metal monolayers.[3-11] In the following section, the important experimental aspects of these in-situ experiments are described, and after this, we explain underpotential electrochemical deposition (UPD), since this is the way the monolayers are deposited. Our results for Tl/Ag(111) are then discussed; we have considered Tl/Ag(111) a prototypical UPD system and have investigated this system in some detail. Following this, we compare the UPD systems of Pb, Tl, and Bi on Ag(111) and Au(111) and draw some general conclusions about the important structure determining-forces in these UPD systems. We then discuss Bi/Ag(111) in more detail, since this system is rather unusual.

2. EXPERIMENTAL ASPECTS

All our experiments were performed in-situ (in an electrolyte) and under potential control. The key to these in-situ experiments is the development of a suitable electrochemical cell. This has been described elsewhere in detail,[4, 5, 10] and here we only briefly mention some important aspects of the cell. The cell is made of Kel-f® and the electrode is clamped to a pedestal that extends slightly above the lip of the cell. A key aspect of the cell design is a thin, flexible polypropylene window that contains the electrolyte above the electrode. The metal monolayers are deposited with the window distended or 'inflated' so a relatively thick (~1mm) layer of electrolyte covers the electrode. The electrolyte is then partially withdrawn and the surface diffraction data are measured through the thin ($\lesssim$30μm) layer of electrolyte that remains on the electrode. This thin-layer geometry minimizes the absorption of the incident and diffracted X rays by the electrolyte and limits the intensity of X rays scattered by the electrolyte (which significantly contribute to the background in these experiments).

The electrode substrates were epitaxially grown Ag and Au thin films that are vapor deposited onto freshly cleaved mica;[4, 5] our data show that these are of high quality.[11] The electrolytes were prepared from ultrapure reagents and "nanopure" (Barnstead), deionized water, and the electrode potentials were measured relative to the Ag/AgCl (3M KCl) reference electrode in the diffraction cell. X-ray data were obtained at the National Synchrotron Light Source (NSLS) beam line X20 with incident X-ray energies of typically 10 keV (wavelengths of 1.24 Å).[8, 9] The X-ray beam was focused onto the sample with a spot size of approximately 1x1 mm^2 and the incident flux was approximately $2x10^{11}$/sec. The incident flux was monitored by a scintillation detector viewing a Kapton foil, and the diffracted intensity was normalized to this monitor count rate to compensate for changes in the incident flux. The diffracted beam was analyzed with 1 mrad Soller slits and the intensity was measured with a scintillation detector.

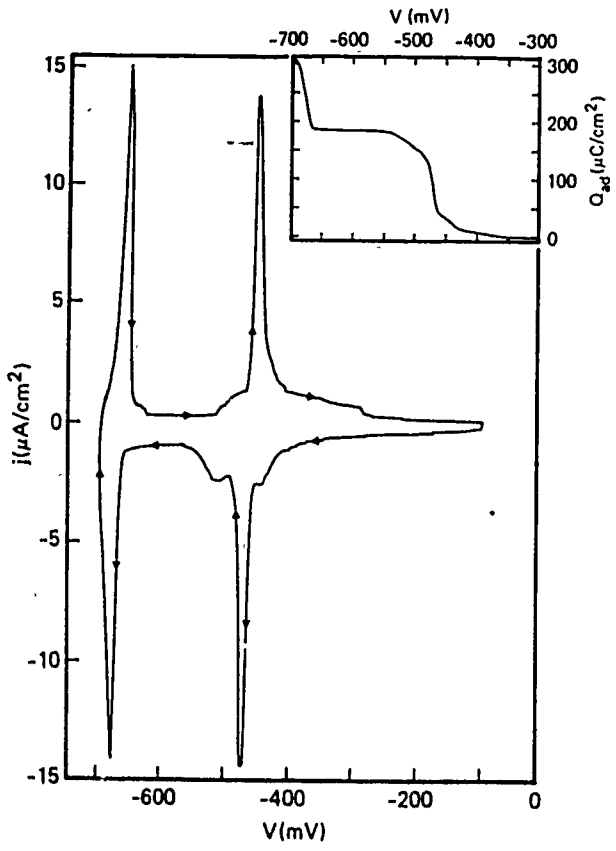

Figure 1. Cyclic voltammogram (CV) for the UPD of Tl on Ag(111) in 2.5x10^{-3} M Tl_2SO_4 and 0.1M Na_2SO_4. The potentials were measured relative to Ag/AgCl (3M KCl) and the scan rate was 2 mV/s. The Nernst potential for bulk deposition is -710mV. The inset shows the adsorption isotherm, which is the integral of the current in the CV. This is the charge, Q_{ad}, that flows into the electrode during Tl deposition. There is a background current due to processes that do not involve Tl deposition. This was estimated by a linear current that passes through the CV at -600 and -180mV. It has been subtracted from the data in the calculation of Q_{ad}.

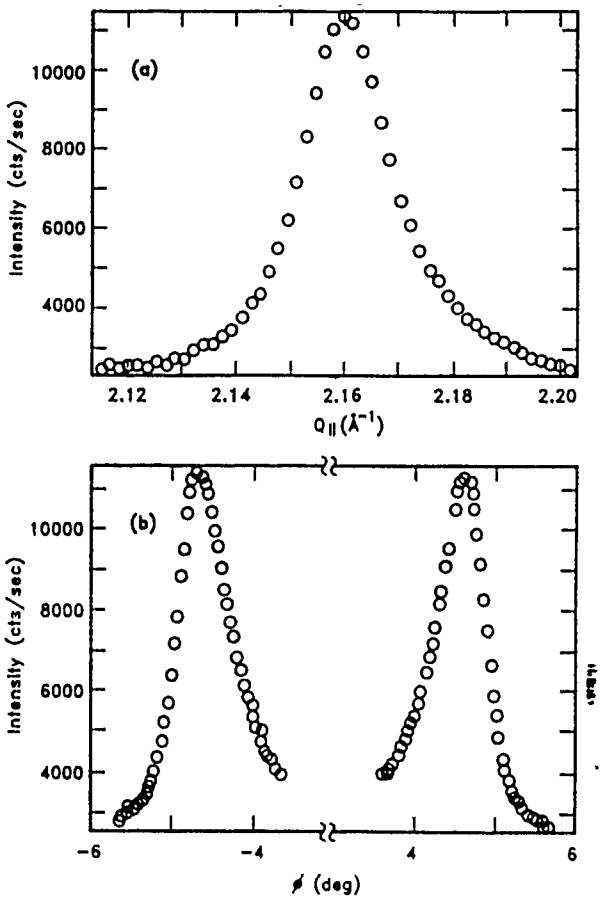

Figure 2. X-ray diffraction of the Tl (10) Bragg rod for Tl/Ag(111) at a deposition potential of -550mV. (a) A radial scan. The azimuthal angle is fixed at $\phi = 4.6°$; this is the angle between the scattering vector and the Ag ($\bar{2}11$) direction. (b) An azimuthal angle scan at fixed $Q_{\parallel} = 2.16$Å^{-1}. In both scans $Q_z = 0.15$Å^{-1}.

3. UNDERPOTENTIAL DEPOSITION

The electrochemical deposition of metal layers onto a foreign metal substrate frequently occurs in distinct stages with the initial formation of one (or more) layers at electrode potentials positive of the Nernst potential for bulk deposition.[15, 16] This process is termed underpotential deposition (UPD), and on single crystals, these initial deposits have been speculated to form well defined, ordered layers.[17] The UPD layers are often deposited by linearly ramping the electrode potential in a negative direction from an initial potential that is positive enough that no metal is adsorbed. Figure 1 shows the current flowing to the Ag electrode during such a linear potential ramp (a cyclic

voltammogram or CV) for Tl on Ag(111).[8, 11, 18, 19] If kinetic effects are absent and the adsorbing ion is completely discharged (as for Tl/Ag(111)[18]), the current flow is proportional to the derivative of the adsorption isotherm.[20] (See the inset in Fig. 1). When the potential reaches -700mV (just positive of the Nernst potential for deposition of bulk Tl), the direction of the potential ramp is reversed and the Tl layers are stripped (or desorbed) from the Ag surface.

The predominant features in Fig. 1 are two sets of large, sharp peaks. The first set occurs at approximately -470mV (240mV positive of the Nernst potential). The peak with negative current results from deposition of Tl, while the positive-current peak is due to stripping. Since the charge associated with deposition (see inset in Fig. 1) is close to that expected for a close packed monolayer of Tl, this negative-current peak has previously been attributed to the deposition of a monolayer of Tl.[18, 20, 21] Correspondingly, the second negative-current peak in Fig. 1 is attributed to the deposition of a second layer of Tl on top of the first, forming a bilayer. Our X-ray scattering measurements confirm these speculations and provide detailed information on the structure of the UPD deposit. In the following sections, we discuss this structure and its dependence on electrode potential.

4.1 MONOLAYER STRUCTURE OF TL/AG(111)

Figure 2 shows radial and azimuthal diffraction scans of the (10) Bragg rod from the Tl monolayer at -550mV. In an azimuthal (or rocking) scan, the diffracted intensity is measured along an arc at a constant scattering vector,[22] $Q = (4\pi/\lambda)\sin\theta$, while in a radial scan, the intensity is measured along a radial scattering vector at constant sample orientation, ϕ. In the radial scan, the intensity is plotted against $Q_{\|}$, the component of the scattering vector parallel to the surface. These data show excellent signal to background, with peak count rates of about 7,500 counts per second (cps) over a background of only 2500 cps. The background is mostly due to scattering from the electrolyte. The azimuthal scan shows peaks at both $\phi = \pm 4.6°$; these two peaks result from two equivalent domains of the Tl monolayer that are oriented $\pm 4.6°$ from the Ag $(\bar{2}11)$ direction.

Figure 3a shows the in-plane diffraction pattern for the Tl monolayer determined from our in-situ X-ray scattering data. In this diffraction pattern, the normal to the substrate is perpendicular to the plane of the paper. The diffraction from both Tl domains was observed with equal intensity and one of the domains is marked with arrows. The diffraction pattern is similar to the LEED pattern that would be observed for Tl/Ag(111), if it were possible to obtain LEED data in an electrolyte. Scans along the Tl (10) and (11) Bragg rods have also been conducted,[9] and provide information about the atomic correlations perpendicular to the surface. In rod scans, the diffracted intensity is measured with $\vec{Q}_{\|}$ held constant, while the component of the scattering vector perpendicular to the substrate surface (Q_z) is varied. From fits to the rod scans, we conclude that the Tl deposit forms a 2D monolayer and that the in-plane and out-of-plane root-mean-square (rms) displacement amplitudes are $\sigma_x = 0.36 \pm 0.05$ Å and $\sigma_z = 0.46 \pm 0.1$ Å, respectively.[9] Note that in addition to dynamic disorder (vibrations), σ_z will include a contribution from any buckling in the monolayer.

The diffraction pattern (Fig. 3a) together with the rod scans show that the Tl deposit forms a 2D incommensurate, hexagonal monolayer in which the adatoms are closely packed together. This structure is almost the same as in the close packed, (00.1) planes of bulk Tl, but the monolayer is compressed compared to the bulk metal and rotated about 4.5° from the Ag $[01\bar{1}]$ direction. Figures 3b and 3c show two schematic representations of the real space structure of one domain of Tl on Ag(111). The open circles represent atoms of the Ag(111) surface and have a diameter proportional to their nearest-neighbor spacing (2.89 Å). The shaded circles represent the Tl adatoms and have a diameter proportional to 3.34 Å, which is approximately their average nearest-neighbor spacing. Figure 3b shows the average structure of the Tl monolayer; it ignores the subtle local modulation in near-neighbor positions that results because the adatoms tend to move toward the lowest energy sites

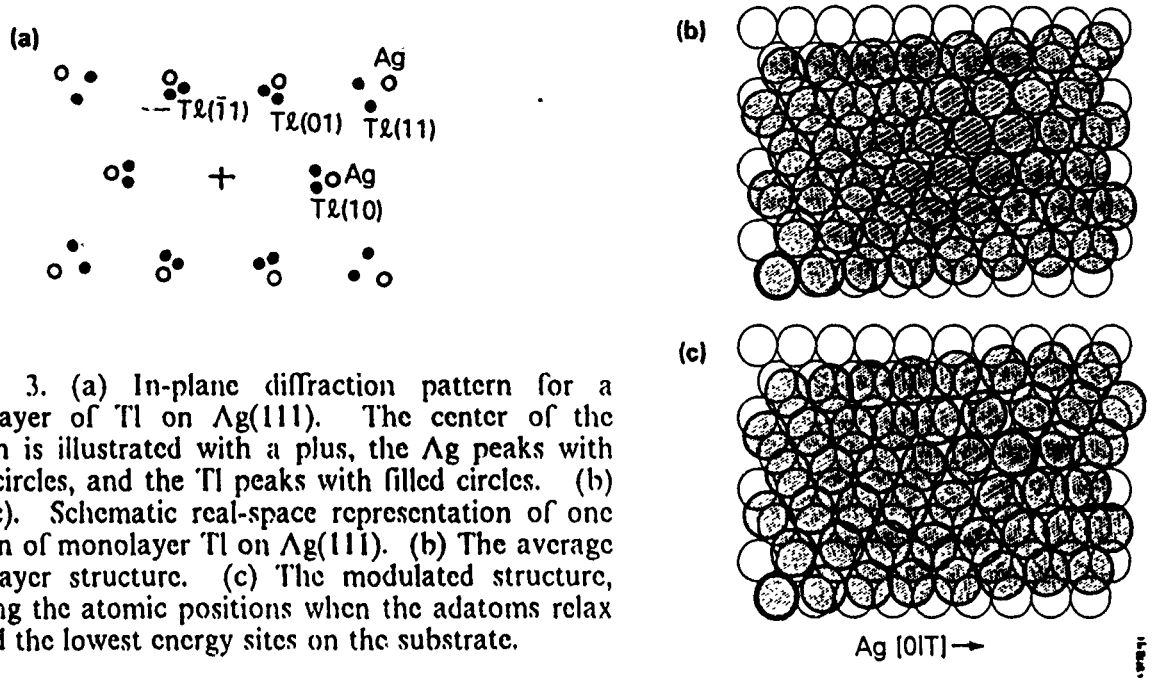

Figure 3. (a) In-plane diffraction pattern for a monolayer of Tl on Ag(111). The center of the pattern is illustrated with a plus, the Ag peaks with open circles, and the Tl peaks with filled circles. (b) and (c). Schematic real-space representation of one domain of monolayer Tl on Ag(111). (b) The average monolayer structure. (c) The modulated structure, showing the atomic positions when the adatoms relax toward the lowest energy sites on the substrate.

on the substrate.[8] We have determined this substrate induced spatial modulation in the Tl monolayer by measuring the intensity changes along the Ag surface rods when the monolayer is deposited, and we find that it has an amplitude of 0.03 Å.[8] The modulation in the incommensurate monolayer changes the intensity of the silver surface scattering, since the modulation has the same periodicity as the silver substrate. The structure of the modulated monolayer is shown in Fig. 3c. The spatial modulation appears as local density increases and decreases that are apparent in Fig. 3c as 'overlapping' adatoms and 'empty spaces' between adatoms, respectively. These density changes increase the monolayer elastic energy, but this increase is more than compensated for by the decrease in the adsorbate-substrate energy that results because the adatoms are in lower energy sites on the substrate.

A dramatic feature of the UPD structure is the large compression of the Tl monolayer compared to bulk Tl. This compression varies with potential (see below), but ranges from 1.4% (at -470 mV) to 3.0% (close to the Nernst potential).[23] Note that a similar compression in bulk Tl would require a pressure of about 50,000 atmospheres. As discussed in Sec. 5, we have also found that UPD monolayers of Pb/Ag(111)[6] and Pb and Tl on Au(111) have similar compressions. These can all be understood with effective medium theory.[11, 24] In this theory, the environment of an atom is modeled as a homogeneous electron gas, and the binding energy of the atom in this environment (e.g., in a solid or at a surface) is related to the embedding energy of the atom in this electron gas. This is the embedding density and it is a monotonically decreasing function of atomic spacing.[24] Thus, in a solid, the minimum in the binding energy as a function of embedding density determines the equilibrium atomic spacing.

If we now consider a free standing monolayer, then the coordination number of the atoms in this layer is less than in a bulk solid. Thus, if the atomic spacing in the monolayer is the same as in the solid, the embedding density of the monolayer is less than the density that gives the minimum binding energy. To reduce the binding energy, the embedding density must increase and this is achieved by a contraction of the atomic spacing (e.g., compression). For the more relevant case of an incommensurate monolayer on a substrate, the substrate atoms will contribute to the embedding

density, and thus, the atomic spacing will be larger than for a free standing monolayer. However, the atomic spacing will still be smaller than bulk, since the coordination number is smaller than in bulk.

4.2 DEPENDENCE OF STRUCTURE ON POTENTIAL

We find that for potentials between -475 and -680 mV, the Tl deposit remains a 2D incommensurate, hexagonal monolayer, but that with decreasing electrode potential, the monolayer compresses. This behavior is shown in Fig. 4, where we plot the dependence of the near-neighbor distance a_{nn} on electrode potential. The datum at -477 mV may represent a metastable state. We observed that the diffraction peak disappeared slowly over about two hours, but after a short initial time ($\simeq$15 minute), the peak position was constant. This potential is very close to the potential where the Tl monolayer is reported to be unstable, transforming into another phase after about 30 minutes.[18, 19] We are continuing to investigate this apparently metastable behavior.

The compression of the monolayer with decreasing electrode potential is readily understood: The chemical potential of the adatoms in the monolayer increases as the electrode potential decreases, because the potential drop across the metal/solution interface becomes more negative (i.e., the driving force to adsorb ions from solution increases). Since the chemical potential of the monolayer has increased, the monolayer free energy can be reduced by increasing the number of Tl adatoms on the Ag surface; this directly leads to the monolayer compression. The compression of UPD layers with decreasing potential is completely analogous to vacuum experiments on the adsorption of rare gases. Here the chemical potential of the adsorbed layer is controlled by the vapor pressure of the gas, and an increase in the vapor pressure causes a compression of the adsorbed layer.[25, 26]

From the dependence of a_{nn} on electrode potential, the 2D isothermal compressibility of the monolayer, κ_{2D}, can be determined.[3, 6, 9] We find that

$$\kappa_{2D} \equiv -\left(\frac{1}{a}\right)\left(\frac{\partial a}{\partial \Phi}\right)_T = -\left(\frac{\partial a}{\partial \mu}\right)_T = \frac{1}{Ze}\left(\frac{\partial a}{\partial V}\right)_T, \tag{1}$$

where Φ is the 2D spreading pressure, a is the atomic area ($\sqrt{3}\, a_{nn}^2/2$ for a hexagonal monolayer such as Tl), μ is the monolayer chemical potential, Z is the number of electrons transferred per atom deposited, and V is the electrode potential.[3, 6, 9] The last identity in Eq. (1) follows because there is chemical and thermal equilibrium between the monolayer and the adsorbing species, and thus, $d\mu = -ZedV$.[15] For metallic adsorbates chemical equilibrium is readily achievable in electrochemical

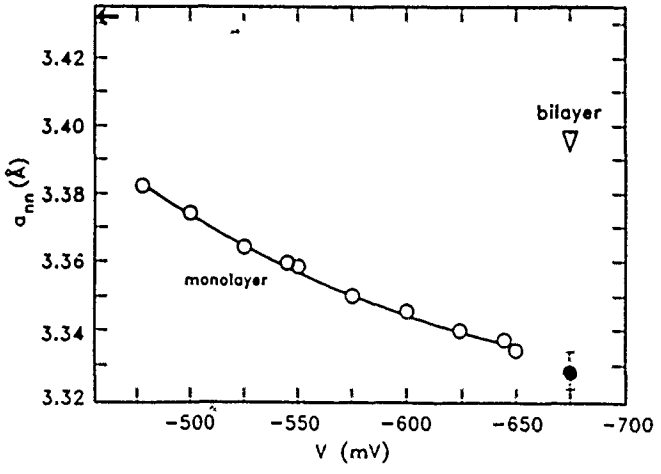

Figure 4. Dependence of the Tl monolayer near-neighbor spacing, a_{nn}, on the electrode potential V. The triangle is for the bilayer and the open circles are for the monolayer. The errors are the size of the data points. The data are plotted as a function of decreasing potential and the line is the least-squares fit of a quadratic to the data. The arrow marks the 'average' near-neighbor spacing for bulk Tl.

environments (where the adsorbing species are ions in solution), but it is almost impossible to achieve chemical equilibrium in vacuum (where the adsorbing species are free metal atoms).

Using Eq. (1) and the derivative of the best-fit quadratic function to the data (shown by the line in Fig. 4), we calculate that for Tl/Ag(111) κ_{2D} varies linearly with potential from 2.2 Å²/eV at -480 mV to 0.9 Å²/eV at -650 mV and that the average compressibility is κ_{2D}= 1.5 Å²/eV. The decrease in the compressibility of Tl/Ag(111) with more negative electrode potentials or smaller near neighbor spacing is expected: As the atomic spacing decreases, the adatom-adatom repulsive force becomes increasingly stronger, and this makes it increasingly difficult to pack the adatoms closer together.

For most bulk metals the compressibility is dominated by the electron compressibility,[27] and hence, a similar domination is expected for metal monolayers. Using a 2D free electron gas model of the compressibility,[3, 6, 27] we estimate κ_{2D}= 0.44 Å²/eV. This is in reasonable agreement with our experiment; in fact, the agreement is as good as that found for a three dimensional free electron gas and bulk Tl. It would be interesting to see if a more realistic value of κ_{2D} could be predicted with a more sophisticated model of Tl on Ag(111), such as an embedded-atom model.[28]

The rotation angle Ω is also dependent on electrode potential.[11] However, we are unable to accurately quantify this behavior, because of an irreversible decrease in Ω with potential cycling. We can, however, determine the qualitative behavior and find that Ω decreases with decreasing near-neighbor spacing (increasing potential). This behavior is consistent with that obtained from the theoretical model of Novaco and McTague, which predicts the dependence of the rotation angle on the near-neighbor spacing for incommensurate adsorbed layers.[29] The rotation of the adsorbed layer away from a high symmetry direction (e.g. Ag [01$\bar{1}$]) results because the rotation allows the adatoms to sit closer to the low energy sites of the substrate and because it takes less energy to create a shear wave (i.e., a rotation) than a compressive wave.[29]

5. A COMPARISON OF UPD MONOLAYERS ON (111) SUBSTRATES

To understand the factors that control the atomic structure of UPD layers, we have studied additional UPD systems: Pb/Ag(111), Bi/Ag(111), Pb/Au(111), and Tl/Au(111). Tl and Pb on Au(111) and Ag(111) form 2D, incommensurate hexagonal monolayers, but Bi/Ag(111) forms a rectangular lattice that is uniaxially commensurate with the hexagonal surface;[9] the structure of the Bi monolayer is described below. For all these UPD systems, we note that the monolayer structure is essentially identical to that for the same vapor deposited system.[4, 5, 11, 30, 31] It is remarkable that in these two very different environments the structure of these metal layers is the same. This shows that for the UPD of these heavy metals (Tl, Pb, Bi) on these smooth (111) surfaces (Ag and Au), the interaction between the solvent molecules and the adatoms does not influence the monolayer structure.

It is reasonable to expect that the structure of a UPD layer could be sensitive to the presence of strongly adsorbing anions, since the anion can influence the nature of the peaks in the CV.[32] Thus, for Pb/Ag(111), we have investigated the monolayer structure in both acetate and perchlorate electrolytes (strongly adsorbing and weakly adsorbing anions, respectively). We find, however, that the monolayer structure and its dependence on potential is the same in both these electrolytes. Similar results are also obtained for Bi/Ag(111) in chloride-containing and chloride-free electrolytes (see below).[9] These observations show that the monolayer structure is not affected by interactions between the adatoms and anions adsorbed on the UPD monolayer.

Since we have found that the structure of the UPD layer is not influenced by the solvent or adsorbed anions, we will now consider the atomic interactions that are important in determining the

monolayer structure for Tl, Pb, and Bi on the (111) faces of Ag and Au. The strongest interaction is that between the adatoms and the substrate, since this bond strength is approximately equal to the adsorbate-adsorbate bond strength plus the UPD shift. Because this interaction is so strong, the UPD deposit forms a monolayer rather than bulk clusters; however, this interaction does not determine the structure within the monolayer. The primary force that determines this structure is the adatom-adatom interaction; we deduce this because the systems adopt structures similar to those found in the closest packed planes of the bulk crystals of the UPD deposits and because the layers are incommensurate. Although the adatom-substrate interaction is strong, the corrugation or spatial variation in the adatom-substrate interaction is rather weak. It influences the structure only weakly by creating the local spatial modulation (see Fig. 3c for Tl/Ag(111)). Note that Bi/Ag(111) is different, since it is commensurate in one direction; this is explained below as a fortuitous match between the substrate and monolayer.

For all UPD layers we have studied, the in-plane spacing between adatoms decreases with decreasing electrode potential. The cause of this change is described above in our discussion of Tl/Ag(111). Our data enable a determination of the 2D compressibilities for these UPD systems. We find that κ_{2D} has average values of 1.8, 1.5, 1.6, and 1.2 Å^2/eV for Tl/Au(111), Tl/Ag(111), Pb/Au(111), and Pb/Ag(111), respectively. Thus, for the same UPD deposit, κ_{2D} is slightly dependent on substrate and is smaller on the Ag(111) than on Au(111), although the reasons for this are not yet clear. If we compare the measured compressibilities to those estimated for the 2D free-electron gas model of the compressibility (see the previous section), we find that this primitive model is in qualitative agreement and correctly predicts the trends.[33] While this is gratifying, the model is not quantitatively correct, and furthermore, it predicts that the compressibility is independent of substrate, in contrast to our observations. It would be interesting to see if a more realistic model could predict the observed compressibilities.

6. BI/AG(111): A RECTANGULAR OVERLAYER AND A TEST OF EX-SITU EMERSION TECHNIQUES

The UPD system Bi/Ag(111) is unusual because the monolayer adopts a *rectangular* structure on a *hexagonal* substrate and because the monolayer lattice is uniaxially commensurate with the Ag substrate along the [$\bar{2}$11] direction.[9] This interesting structure is shown in Fig. 5. Another unusual aspect of this UPD layer is that the structure has the two Bi adatoms per rectangular unit cell, but it is not a centered-rectangular lattice. From surface crystallographic measurements, we find that the nearly-centered adatom is displaced from the centered position by 0.35 Å along the commensurate direction (see Fig. 5). This displacement shortens two of the Bi-Bi near-neighbor bond distances but lengthens two others and likely reflects the tendency toward covalent bonding in Bi. The monolayer structure is quite close to that of the close-packed or (102) planes of bulk hexagonal Bi, and this supports our conclusion that the primary force that determines the structure of the UPD layer is the adatom-adatom interaction. We believe that the commensurate nature of the Bi monolayer is due to a fortuitously close match between the atomic spacings of the Ag substrate and the (102) Bi planes.[33]

Our surface crystallographic measurements also show that the disorder in the monolayer is anisotropic: the rms displacement amplitude in the commensurate direction is 0.2 Å, while in the incommensurate direction, it is 0.3 Å. This reflects the tendency of the substrate to 'lock' the adatoms in position along the commensurate direction. In addition, we have used measurements of the intensities of the Ag surface diffraction to determine the registry of the Bi[10] rows. Since the Bi is commensurate with the Ag (in one direction), its diffraction interferes with the Ag diffraction and this can be used to determine the registry. Our measurements indicate that the Bi[10] rows lie along the rows of three-fold hollow sites on the Ag surface. This is reasonable, since these hollow sites are likely the minimum energy sites. (We have shown this for Tl/Ag(111).)[8]

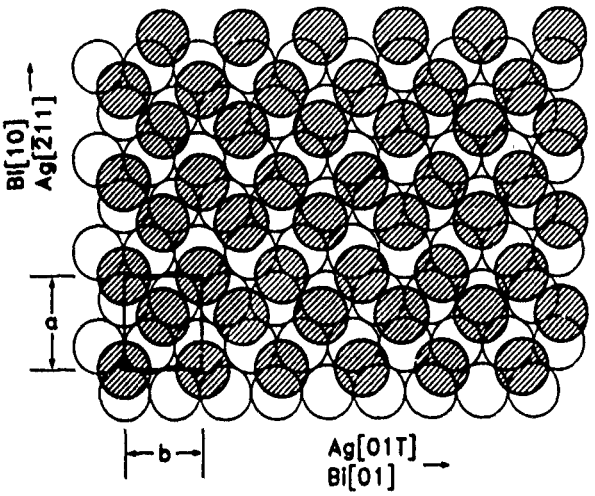

Figure 5. Structure of UPD Bi/Ag(111). The open circles represent the surface atoms of the Ag substrate and the shaded circles represent the Bi adatoms. The relative sizes of these circles correspond to the near neighbor spacing of bulk Ag (2.89Å) and bulk Bi (3.07Å). The Bi monolayer is commensurate in the a direction, (a = 5.005Å = $\sqrt{3}$ times Ag nearest-neighbor distance), but is incommensurate in the b direction (b = 4.48Å - 4.56Å).

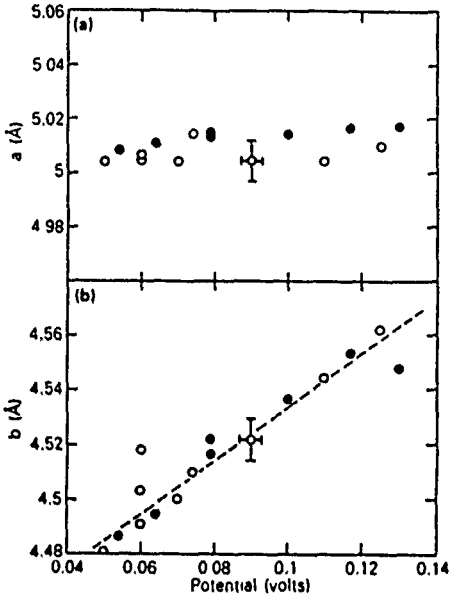

Figure 6. Dependence of the Bi monolayer lattice constants on the electrode potential V. The filled and open circles are for chloride-free (0.1M $HClO_4$ with 2.5mM Bi_2O_3) and chloride-containing (0.1M $HClO_4$ with 2.5mM Bi_2O_3 and 0.35mM NaCl) electrolytes, respectively. (a) The lattice constant, a, which has an average value of $a = 5.007 \pm 0.002$Å. (b) The lattice constant b. The line is a linear least-squares fit to the data.

The potential dependence of the structure of UPD Bi/Ag(111) is interesting. In contrast to Tl and Pb, where the monolayers compress isotropically as the electrode potential decreases, Bi compresses *uniaxially* along the incommensurate direction (Ag[01$\bar{1}$]). This is demonstrated in Fig. 6, where the a and b lattice constants of the monolayer are plotted vs potential in both chloride-containing and chloride-free electrolytes. In both electrolytes only the incommensurate lattice constant, b, depends on the electrode potential. The commensurate lattice constant, a, remains locked to the Ag lattice over the entire potential range where the monolayer is stable. Thus, the compression preserves the uniaxial commensurate structure. The compressibility that we calculate from Fig. 6 and Eq. (1) is $\kappa_{2D} = 0.8$ Å^2/eV. As expected, this is about the same for UPD monolayers of Tl and Pb and is in reasonable agreement with κ_{2D} for a 2D free electron gas ($\simeq 0.2$Å^2/eV). We note that although the compression is uniaxial, the compressibility we measure is a *two-dimensional* compressibility, not a one-dimensional compressibility, since the monolayer is inherently two dimensional.

Our Bi/Ag(111) experiments also permit direct comparison of a surface structure determined in-situ with the structure measured 'ex-situ', after emersion (removal) from an electrochemical cell.[9] Because of the lack of in-situ techniques for studying adsorbed layers at solid-liquid interfaces, considerable effort has been directed toward studying these layers using ex-situ techniques, where the electrode surface is examined with surface science methods following emersion of the electrode.[34-36] One of the key questions to be addressed is whether the structure determined ex-situ (after emersion) is the same as the structure in-situ. Thus, we have compared our structure for Bi/Ag(111) to the

surface structure measured by ex situ methods (LEED)[36] and we find that the structures are the same.[9] This provides an important existence proof that the in-situ monolayer structure can be preserved in ex-situ emersion experiments.

7. SUMMARY

We have described results of in-situ surface X-ray scattering experiments on electrochemically deposited layers of Pb, Tl, and Bi on Ag and Au (111) electrodes. Tl and Pb form 2D, incommensurate hexagonal monolayers that are compressed compared to bulk and rotated by 4-5° with respect to the substrate. The compression is interpreted in terms of effective medium theory.[24, 37] As the electrode potential decreases, the in-plane atomic spacing also decreases, and these data enable the determination of the monolayer compressibility. For both Tl and Pb, the compressibility is depends only weakly on substrate and is smaller on Ag(111) than on Au(111). The observed compressibilities are in reasonable agreement with those calculated for a 2D free electron gas model. For Tl/Ag(111), we have measured the substrate-induced modulation of the atomic positions in the monolayer and find that it is small. Bi/Ag(111) is unusual and forms a rectangular lattice that is uniaxially commensurate with the substrate. The commensurate Bi rows lie along the rows of three-fold hollow sites and there are two Bi adatoms per rectangular unit cell. This unusual structure reflects both the tendency toward covalent bonding in Bi and a match between the atomic spacings of the Ag substrate and the (102) planes of bulk Bi. In contrast to Tl and Pb, Bi/Ag(111) compresses anisotropically to maintain the uniaxial commensurate structure. A comparison between the in-situ and ex-situ structures of UPD Bi/Ag(111) demonstrates that the in-situ monolayer structure can be preserved in ex-situ emersion experiments.

Our results show that for these metal monolayer systems the adatom-adatom interactions predominantly determine the atomic structure of the monolayer. The adatom-substrate interactions only weakly influence this structure and the presence of the large concentration of adsorbed water molecules or adsorbing anions do not affect the structure. These experiments also show the surface X-ray scattering can provide important, microscopic information on the structure of solid-liquid interfaces.

ACKNOWLEDGMENTS

We gratefully acknowledge the assistance of our collaborators Gary Borges, Mahesh Samant, Larry Sorensen, Dave Wiesler, and Dennis Yee, and we thank Jean Jordan-Sweet and Brian Stephenson for their assistance with beam line X20. This work was partially supported by the Office of Naval Research. It was performed at the National Synchrotron Light Source, Brookhaven National Laboratory, which is supported by the U.S. Department of Energy, Division of Material Sciences and Division of Chemical Sciences.

REFERENCES

1. P. Eisenberger and W.C. Marra, Phys. Rev. Lett. 46, 1081 (1981).
2. R. Feidenhans'l, Surf. Sci. Reports 10, 105 (1989).
3. M.F. Toney and O.R. Melroy, in *In-Situ Studies of Electrochemical Interfaces*, edited by H.D. Abruna (VCH Verlag Chemical, Berlin, 1991).
4. M.G. Samant, M.F. Toney, G.L. Borges, L. Blum, and O.R. Melroy, Surf. Sci. 193, L29 (1988).
5. M.G. Samant, M.F. Toney, G.L. Borges, L. Blum, and O.R. Melroy, J. Phys. Chem 92, 220 (1988)
6. O.R. Melroy, M.F. Toney, G.L. Borges, M.G. Samant, J.B. Kortright, P.N. Ross, and L. Blum, Phys Rev. B 38, 10962 (1988).

7. O.R. Melroy, M.F. Toney, G.L. Borges, M.G. Samant, J.B. Kortright, P.N. Ross, and L. Blum, J. Electroanal. Chem. **258**, 403 (1989).
8. M.F. Toney, J.G. Gordon, L.S. Kau, G. Borges, O.R. Melroy, M.G. Samant, D.G. Wiesler, D. Yee, and L.B. Sorensen, Phys. Rev. B **42**, 5594 (1990).
9. M.F. Toney, J.G. Gordon, M.G. Samant, G.L. Borges, D.G. Wiesler, D. Yee, and L.B. Sorensen, Langmuir **7**, 796 (1991).
10. M.F. Toney, in *The Application of Surface Analysis Methods to Environmental/Materials Interactions*, edited by D.R. Baer, C.R. Clayton, and G.D. Davis (The Electrochemical Society, Pennington, 1991), p. 200.
11. M.F. Toney, J.G. Gordon, G. Borges, O.R. Melroy, M.G. Samant, D.G. Wiesler, D. Yee, and L.B. Sorensen, submitted to Surf. Sci., 1991.
12. M.J. Bedzyk, G.M. Bommarito, M. Caffrey, and T.L. Penner, Science **248**, 52 (1990).
13. B. Ocko, J. Wang, A. Davenport, and H. Isaacs, Phys. Rev. Lett. **65**, 1466 (1990).
14. C.A. Melendres, H. You, V.A. Maroni, Z. Nagy, and W. Yun, J. Electroanal. Chem. **297**, 549 (1991).
15. D. Kolb, M. Przasnyski, and H. Gerischer, J. Electroanal. Chem. **54**, 25 (1974).
16. D.M. Kolb, in *Advances in Electrochemistry and Electrochemical Engineering*, edited by H. Gerischer and C.W. Tobias (Wiley, New York, 1978), Vol. 11, p. 125.
17. D.M. Kolb, J. Vac. Sci. Technol. A **4**, 1294 (1986).
18. H. Siegenthaler, K. Juttner, E. Schmidt, and W.J. Lorenz, Electrochim. Acta **23**, 1009 (1978).
19. K. Juttner and H. Siegenthaler, Electrochim. Acta **23**, 971 (1978).
20. W.J. Lorenz, H.D. Hermann, N. Wuthrich, and F. Hilbert, J. Electrochem. Soc. **121**, 1167 (1974).
21. A. Bewick and B. Thomas, J. Electroanal. Chem. **65**, 911 (1975).
22. The scattering vector is the difference between the incoming and diffracted X-ray wavevectors.
23. To compare three dimensional TI with 2D TI, we quote the compression in terms of the difference in near-neighbor spacing.
24. K.W. Jacobsen, Comments Cond. Mat. Phys. **14**, 129 (1988).
25. C.G. Shaw and S.C. Fain, Surf. Sci. **91**, L1 (1980).
26. J. Unguris, L.W. Bruch, E.R. Moog, and M.B. Webb, Surf. Sci. **109**, 522 (1981).
27. N.W. Ashcroft and N.D. Mermin, *Solid State Physics* (Saunders College, Philadelphia, 1976).
28. M.S. Daw and M.I. Baskes, Phys. Rev. B **29**, 6443 (1984).
29. J.P. McTague and A.D. Novaco, Phys. Rev. B **19**, 5299 (1979).
30. K.J. Rawlings, M.J. Gibson, and P.J. Dobson, J. Phys. D **11**, 2059 (1978).
31. J. Perdereau, J.P. Biberian, and G.E. Rhead, J. Phys. D **4**, 798 (1974).
32. V.D. Jovic, B.M. Jovic, and A.R. Despic, J. Electroanal. Chem. **288**, 229 (1990).
33. M.F. Toney, J.G. Gordon, G. Borges, D.G. Wiesler, D. Yee, and L.B. Sorensen, unpublished, 1991.
34. A.T. Hubbard, Acc. Chem. Res. **13**, 177 (1980).
35. P.N. Ross, Surface Sci. **102**, 463 (1981).
36. L. Laguren-Davidson, F. Lu, G.N. Salaita, and A.T. Hubbard, Langmuir **4**, 224 (1988).
37. K.W. Jacobsen, J.K. Norskov, and M.J. Puska, Phys. Rev. B **35**, 7423 (1987).